Alternate-Fueled Combustor-Sector Performance: Part A: Combustor Performance Part B: Combustor Emissions

D.T. Shouse,[1] C. Neuroth,[1] R.C. Hendricks,[2] A. Lynch,[1] C. Frayne,[1] J.S. Stutrud,[1] E. Corporan,[1] Capt. T. Hankins[1]

[1]AFRL/WPAFB
Wright-Patterson Air Force Base, Ohio 45433, USA
E-mail: dale.shouse@wpafb.af.mil

[2]NASA Glenn Research Center, Cleveland, Ohio 44135, USA

ASBTRACT

Alternate aviation fuels for military or commercial use are required to satisfy MIL-DTL-83133F(2008) or ASTM D 7566 (2010) standards, respectively, and are classified as "drop-in" fuel replacements. To satisfy legacy issues, blends to 50% alternate fuel with petroleum fuels are certified individually on the basis of feedstock. Adherence to alternate fuels and fuel blends requires "smart fueling systems" or advanced fuel-flexible systems, including combustors and engines without significant sacrifice in performance or emissions requirements. This paper provides preliminary performance (Part A) and emissions and particulates (Part B) combustor sector data for synthetic-parafinic-kerosene- (SPK-) type fuel and blends with JP-8+100 relative to JP-8+100 as baseline fueling.

INTRODUCTION

Synthetic and biomass fueling are now considered as near-term aviation alternate fueling. The major impediment is a secure sustainable supply of these fuels at reasonable cost. Alternate aviation fuels are currently required to satisfy MIL-DTL-83133F(2008) for Fisher-Tropsch- (FT-) equivalent processed ASTM D 7566 (2010) and known as "drop-in" fuel replacements (military and civil, respectively). As in aviation, many land-based and marine power generation systems are elderly, known as the legacy issue. Fueling these systems requires careful compliance to the fuel handling and engine systems for which they were (are) designed. To satisfy a sustainable fuel supply, it will be necessary to accept fuels derived from a variety of feedstocks. Consequently, adherence to alternate fuels and fuel blends requires "smart fueling systems" or advanced fuel-flexible systems, including combustors and engines without significant sacrifice in performance or emissions requirements.

For many diesel systems biomass derived oils are unsuitable because sufficient aromatics and sulfur are lacking which provide lubricity thus reducing design component life. To counter these issues, additives are promoted.

This paper provides preliminary performance, emissions and particulates combustor sector data relative to JP-8+100 as baseline fueling, for SPK-type fuels blends (herein FT-type fuel) and projections for testing of biofuel fuel blends leading to preliminary development of smart fueling (fuel flexible) and combustor systems for the next generation aeronautic and aeronautic-derivative gas turbine engines.

Truly performance and emissions are coupled issues; however, combustor performance will be presented in Part A and combustor emissions as Part B for understanding both in sufficient detail.

PART A: COMBUSTOR PERFORMANCE

Part A presents fueling characteristics, facility development, and operation followed by thermal performance of the combustor and combustor visualization. Herein denoted as combustor A, the results are for one of several combustors to be evaluated in development of fuel-flexible engine combustors.

Most data herein are testing at nominal inlet conditions of 225 psia and 800 °F (1.55 MPa, 700 K) at 3% combustor pressure drop, where JP-8+100 (JP-8) is taken as baseline. Selected emissions data are provided at and below 225 psia (1.55 MPa).

FUEL CHARACTERISTICS

In general all alternate fueling is required to meet or exceed MIL-DTL-83133F or ASTM D7566 requirements. The carbon-distribution for each fuel used and primary characteristics differ depending on feedstock source and distilling practices, yet all fall within specification. Typical C-distributions for JP-8 and an (SPK) FT-derived fuel are shown in Fig. 1a with vendor variations in fuels illustrated in Fig. 1b. Secondary refining of petroleum-based kerosene fuels can also satisfy specifications.

The specifications for one of the fuels, AFRL No. 5172 Shell GTL-SPK (FT), is presented in Appendix A.

COMBUSTOR AND FACILITY CHARACTERISTICS

The general description of the combustor and supporting research cell data are similar to those reported in Hendricks et al. (2004). The particular aspects of the geometry tested are proprietary and will not be discussed herein. Details of the High Pressure Combustion Research Facility at the Air Force Research Laboratory (AFRL) are provided in Shouse et al. (2001).

Although some general aspects of the fuel delivery system and operations of the facility are similar to that in Hendricks et al. (2004), specific facility modifications and increased capability to handle fuel blending had to be made, including remote alternate test fuel storage/tankage and delivery of the alternate test fuel to the facility fuel pumps, flow meters, and control systems.

Facility Development

Before validation data could be taken, it was necessary to learn what it takes to conduct high-pressure combustor testing of alternate fuels such as FT and biomass feedstock fuels. It is first necessary to establish the combustion parameters required by the study such as operability, performance, durability time-dependent measurements such as flame studies and others. Next, an assessment of the effects of pressure ratios and inlet temperatures on both the combustor sector model and desired data was undertaken as well as most importantly, how to safely blend the fuels. The blending system, while complex, enables operations to establish and stabilize combustor inlet pressures and temperatures of preheated air at the required test condition without the additional complication of simultaneously establishing fuel blend.

To establish the fuel delivery system, questions such as how much fuel and time are required to fully evaluate a typical fuel candidate must be resolved. A 500-gal trailer-mounted fuel tank was chosen for porting alternative fuels with the added feature of coupling to the facility fueling system. The facility has two duplicate fuel systems that provided a means of handling JP-8 fuel with one system to pump, meter, and control the JP-8 fuel; this system is referred to as the main fuel delivery system. The identical system was fed the alternative fuel supply, which is pumped from the trailer into the facility primary fuel system and ultimately blended online with the main fuel system to provide the desired fuel blend from 0% to 100% trailer fuel.

Test Parameters and Data Collection

For this series of testing, the nominal test conditions for pressures and temperatures of blends and the extensive data collection systems have been established. The parameters were chosen to be most representative of engine operations envelope from idle to altitude cruise; however, TO (take-off) pressures are currently beyond the range of this facility.

Combustor parameters

Inlet pressures (P): 75, 125, 175, and 225 psia (0.517, 0.862, 1.207, and 1.551 MPa)
Inlet temperature (T): 500, 625, 725, and 790 °F (533, 603, 658, and 694 K)
Combustor pressure drops (ΔP): 3%, 4%, and 5%
Fuel blends: 100% JP-8, 50:50 JP-8:FT, and 100% FT

Data collection

Gaseous emissions
Exit temperature rake type B thermocouples, (also for metal and sidewall temperatures)
Photo diode output (voltage)
Still and high-speed photography
Smoke and particulate emissions

Combustor outer and inner liner temperature data are given in Appendix B.

COMBUSTOR THERMAL PERFORMANCE

The combustion efficiencies for combinations of fuel:air ratio F/A and fuel compositions were of the order of 99.9% (Table. 1), and one is unable to distinguish combustor changes from this single parameter; thus, other parameters will be investigated. For example, the calculated flame temperature (Fig. 2) increases with F/A, with FT about ΔT = 70 °F (39 K) higher.

Lean blow out (LBO) tests were conducted and found consistent with JP-8+100, and no further tests were undertaken. Altitude restart tests are yet to be conducted.

SURFACE THERMAL MEASUREMENTS

The combustor walls and liners were instrumented for pressure and temperature. In general the pressure drop measurements are sensitive information and will not be presented as such. It should be noted that no inconsistent pressure measurements were found.

The liner and wall surface temperature locations are sensitive information and temperatures are noted as sidewall or liner (i.e., facing inside or outside).

For all figures herein, fuel compositions are denoted as follows: JP-8+100 is JP-8, Fischer-Tropsch is FT, and blended 50% JP-8+100 and 50% FT by volume is 50:50.

Sidewalls

Figure 3 illustrates that sidewall temperatures (TSW) strongly depend on F/A and weakly depend on fuel blend composition JP-8, FT, and 50:50. FWD represents forward; MID, middle; and AFT, the aft axial position of the thermocouple.

Unwrapped Combustor Liner

Figures 4a, b, and c represent unwrapped liner surface temperatures for three F/A values (0.010, 0.015, and 0.020) and three fueling compositions (JP-8, FT, and 50:50). The twin peaks represent sidewall (largest) and maximum inner liner temperatures, respectively.

Figure 4a illustrates the unwrapped liner temperatures for F/A = 0.010 with outer liner temperatures to the left of the peak and inner liner temperatures to the right of the peak. The temperatures are slightly higher for the FT fueling.

Figure 4b represents unwrapped liner temperatures for F/A = 0.015 with outer liner temperatures to the left of the peak and inner liner temperatures to the right of the peak. The temperatures are lower for the FT fueling.

Figure 4c represents the unwrapped liner temperatures for F/A = 0.020 (JP-8) and 0.019 (FT) with outer liner temperatures to the left of the peak and inner liner temperatures to the right of the peak. The temperatures are lower for the FT fueling.

Figure 5 shows that peak inner liner temperatures are nearly independent of fueling composition from 100% JP-8 to 100% FT.

Combustor Inner and Outer Liner

Eliminating the sidewall peak temperature allows visualization of the smaller changes in surface temperatures. Omitting the peak temperature, Figs. 6a through 6f illustrate major portions of the combustor liner axial and circumferential surface temperature variations with F/A and fueling composition.

Figures 6a and b illustrate variations of combustor axial and circumferential surface temperatures. Figure 6a shows inner liner temperatures at F/A = 0.010 for fueling composition changes from JP-8 to FT. The temperatures for FT and blended fueling are slightly higher than for JP-8 fueling. Figure 6b shows variations of outer liner combustions temperatures at F/A = 0.010 for

fueling composition changes from JP-8 to FT. The temperatures for FT and blended fueling are slightly higher than for JP-8 fueling.

Figure 6c shows variations of combustor outer liner temperatures at F/A = 0.015 for fueling composition changes from JP-8 to FT. Figure 6d illustrates variations of combustor inner liner temperatures at F/A = 0.015 for fueling composition changes from JP-8 to FT.

Figure 6e shows variations of combustor inner liner temperatures at F/A ~0.020 for fueling composition changes from JP-8 to FT. Figure 6f shows variations of combustor outer liner temperatures at F/A ~0.020 for fueling composition changes from JP-8 to FT.

COMBUSTION VISUALIZATION

High-speed photographs of the combustion process provide some insights for computational fluid dynamics (CFD) analysts as well as heuristic information for combustor designers: for example, decreased luminosity with FT versus JP-8. The proprietary nature of the combustor being tested makes it difficult to provide photographs and high-speed video of the combustor process requiring most details to be withheld, and it will not be discussed further.

CONCLUSIONS: PART A

Alternate fueling testing is being carried out to determine preliminary performance, emissions, and particulates combustor sector data for SPK-type (e.g., Fischer-Tropsch) fuel blends, relative to JP-8+100 as baseline fueling, and to make projections for testing of biofuel fuel blends leading to preliminary development of smart fueling (fuel flexible) and combustor systems for the next generation aeronautic and aeronautic-derivative gas turbine engines. Herein alternate fueling test results for a well-characterized but proprietary combustor are provided for JP-8+100 and a Fischer-Tropsch- (FT-) derived fuel and a blend of 50% each by volume.

The test data presented are part of a more extensive data set where combustion parameters were varied over a range of values. The data herein are for the case of nominal inlet conditions at 225 psia and 800 °F (1.551 MPa and 700 K), and JP-8+100 is taken as baseline. These data provide the following results:

1. Combustor performance efficiencies at 0% FT (JP-8), at 50% blended FT and JP-8, and at 100% FT are nearly identical at about 99.9%
2. Both outer and inner wall temperatures run
   a. warmer at F/A = 0.010 by at most 9 °F with FT fueling
   b. cooler at F/A = 0.015 by at most 50 °F with FT fueling
   c. cooler at F/A=0.02 (0.019) by at most 80 °F with FT fueling
3. Center peak liner temperatures nearly the same to within $\Delta T = 10$ °F (5.55 K)
4. Rake temperatures show core flow generally higher with FT than JP-8, but one rake thermocouple (TC) was lost during testing, which inhibits conclusiveness.
5. All temperatures increase with F/A.
6. The 50:50 blend test results generally are between JP-8 and FT and somewhat closer to FT.
7. LBO testing results show no change in LBO with FT from JP-8.
8. Altitude relight testing remains to be carried out.
9. High-speed photographs of the combustion process provide some insights for CFD analysts as well as heuristic information for combustor designers. For example, there was decreased luminosity with FT versus JP-8, and clips show enhanced vorticity for the conditions cited in Table. 1.

PART B: COMBUSTOR EMISSIONS

Part B presents gaseous emissions as CO_2, CO, and NOx (which also includes smoke and luminosity data); particulate emissions including distribution; and a brief comparison to small and large engine testing results from other programs. The emissions data are taken for the same tests and test conditions cited in PART A, nominally 225 psia at 800 °F (1.551 MPa at 700 K) with the sampling probe located at the nozzle exit plane. Emissions have a direct impact on aviation climatic constraints based on life cycle analysis (LCA) of fueling feedstocks, which includes fueling development and engine emissions. Herein the testing is directed toward fuel flex engine combustors, providing basic data for LCA fueling evaluations, where combustor A is one of several to be evaluated in development of fuel-flexible engine combustors.

GASEOUS EMISSIONS

Measurements for NOx were determined from combining NO and NO_2 measurements (Figs. 7a and b). Nitric oxide (NO) with molecular atomic dimension (0.115 nm) (NO), while less than JP-8 at F/A = 0.010, steadily increases to become marginally higher than JP-8 at F/A = 0.020 (extrapolated) (Fig. 6a). Nitrogen dioxide (NO_2) (0.221 nm) (ppm) for FT or 50:50 blended fueling is considerably higher than for JP-8 and generally increases with F/A. Combining nitrogen dioxide (ppm) and nitric oxide (ppm), the trend with F/A and fuel composition is similar to that seen for NO; less than JP-8 at F/A = 0.010 and marginally higher than JP-8 at F/A = 0.020 (Fig. 7c)

The variation of $\%CO_2$ (0.0116 nm), ppm CO, and $\%O_2$, (Figs. 8, 9, and 10), while strongly increasing with F/A, are marginally consistent with varied dependencies on fuel composition. The $\%CO_2$ appears somewhat consistent with decreased %CO and O_2 with fueling changes from JP-8 to FT, in agreement with flame temperature (Fig. 2).

Figure 8 shows the strong variation of $\%CO_2$ with F/A, but it is nearly independent of fuel composition. However, it appears somewhat consistent with decreased $\%O_2$ with fueling changes from JP-8 to FT. Carbon monoxide (0.113 nm) (CO) generally is lower with fueling from JP-8 to FT with some changes at F/A = 0.019, which extrapolated is unresolved (Fig. 9). The decrease in $\%O_2$ (Fig. 10) is consistent with increasing F/A—as well as higher rake temperatures—with FT, indicating increased combustion temperatures with more complete combustion (Fig. 2).

SMOKE AND PHOTO DIODE NUMBERS

The general trend of total hydrocarbon emissions (THC) (Fig. 11) strongly depends on fuel:air ratio F/A and is less dependent on fuel blend except with FT at F/A = 0.015. The reason is not known at this time, nor is it entirely clear that for all intensive purposes why THC is nearly independent of fuel composition because the smoke data do show more distinctive trends with fueling composition at F/A = 0.010 (Fig. 12). For FT fueling, the smoke number is well below that of JP-8 at F/A of 0.01 and 0.02, yet they are nearly the same at F/A = 0.015. FT smoke number increases with F/A, but it is not clear for either JP-8 or 50:50 blended fuel.

Smoke number and THC results reinforce the necessity for good particulate measurements, their distribution, composition, and toxicology.

Figure 13 illustrates the change in flame luminosity on a relative basis as the blend of JP-8 and FT fuel is varied. Optical access windows are combustor pressure limited, and the data set shown is at $(P,T)_{inlet}$ (75 psia (0.517 MPa), 500 °F (533 K)) at 3% combustor pressure drop.

The increase in flame luminosity follows the same trends for collected smoke data as shown in Fig. 14. The decline in smoke number with increasing FT fueling is most pronounced at lower F/A ratios. Smoke number consistently increases with F/A independently of fueling yet is lowest at 100% FT fueling. A striking feature is the decrease in relative flame luminosity as illustrated in Fig. 13 with the characteristic clean blue flame at 100% FT fueling. This increase in smoke number and flame luminosity as the fuel blend is increased to 100% JP-8 suggests that the radiative heat load on the combustor increases as well at higher F/A ratios; the wall metal temperatures corroborate this increase.

Figure 14 illustrates a decrease in smoke number as combustor pressure changes from 175 to 225 psia (1.207 to 1.551 MPa) (note the anomaly at 175 psia (1.207 MPa)) with consistent increases in smoke number and photo diode emissions with increased F/A from 0.020 to 0.025. In general these trends corroborate the particulate data shown later.

PARTICULATE EMISSIONS

The particulate distribution depends on engine power setting, pressure, F/A and fueling composition, and the chemical nature of the particulates and their toxicity. Such data are necessary for determination of environmental health hazards, cloud formations, and climatic changes.

To demonstrate the operability of the emissions probes, the test F/A ratios were compared with the CO_2-based F/A ratios. The 100% FT and 50:50 blends are within +12% to –18% of one-to-one correspondence whereas the 100% JP-8 is +8% to –34% with one point at –50%. The general trends are for FT and blends to be consistently higher and JP-8 lower than one-to-one correspondence (Fig. 15). Such evidence may reflect the paraffinic nature of FT and the high aromatic and cyclohydrocarbon content of JP-8.

The nitrogen gas tip-diluted, water-cooled particulate probe is illustrated in Fig. 16. Because of in-plane hardware details, the photo and detail insert are shown rotated out of true exhaust plane. The probe cap outer diameter = 0.075 in. (19 mm) with aperture diameter 0.044 in. (1.12 mm). The probe aperture aspirated exhausted gas steam is quenched by water cooling, which also prevents probe failures from overheating. Both diluted and undiluted probes were positioned at the combustor exhaust plane. For the dilution probe, the exhaust gas is further cooled and diluted with nitrogen gas. Both types are held above condensation temperature of water and organics en route to the instrumentation sampling panel. Details of the facility and gas emissions sampling probes are given in Shouse et al. (2001).

In terms of particle emissions indices EI_n, the general trends with both pressure and F/A are higher EI_n values (number/kg-fuel burn) for JP-8 and lower values for FT with the 50% blend (50% JP-8 and 50% FT) in between (Fig. 17). At an F/A of 0.015, the FT emissions index EI_n –FT is nearly ¼ that of JP-8 at 175 psia (1.207 MPa); at F/A = 0.020, nearly ½ at 225 psia (1.551 MPa); and at F/A = 0.025, nearly 7/8 at 175 psia (1.207 MPa). Note, however, the variability of 50% fuel blend at lower pressures of 75 psia (0.517 MPa). Whereas it is difficult to make a direct comparison with on-wing engine testing, the data trends are consistent where FT particulate emissions are much lower than Jet A at low power (lower engine pressure), yet the difference trend diminishes with increased engine power (higher engine pressure).

Trends with the cleaner paraffinic fuels (FT) are also reflected in terms of particulate size distribution (Fig. 18) but not necessarily in terms of the FT blend, where at 75 psia (0.517 MPa) anomalous behavior is observed, namely the number of particulates (N) of size Dp (equivalent diameter) per cubic centimeter increases beyond that of JP-8. However for FT fueling, the values of the $[dN/d(\log D_p)]$ derivative indicate the total particle counts (integrals) are nearly half that of JP-8. Note the peak shift toward smaller diameter particulates, and the smaller (about half the size of the JP-8 peak) particulates making more difficult to detect, isolate, collect and dispose of such particulates. Further, the toxicology requires much study.

Particulate size and to some extent, distribution, are highly dependent on the probe. Effects of probe tip dilution and probe secondary dilution are illustrated in Fig. 19 for combustor pressure of 125 psia (0.862 MPa) and F/A = 0.015. Here the trend with particulate size is not as definite as illustrated in Fig. 18, and the effects of probe dilution diminishes with fuel blending.

Looking again at the anomalous trends at combustor pressure of 75 psia (0.517 MPa) and 175 psia (1.207 MPa) shown in Figs. 17 and 18, shows similar trends in particulate distribution (Fig. 20). Whereas the cleaner FT fuel particulate peak is still less than that of JP-8 or the FT blend, the trend is minor by comparison with those shown in Fig. 17 at other pressures. While consistent, the behavioral reasons remain to be explored.

In contrast to the distribution trends at combustor pressure of 75 psia (0.517 MPa) and 175 psia (1.207 MPa) and F/A = 0.025 (Fig. 20), the trends at combustor pressure of 225 psia (1.551 MPa) and F/A = 0.020 are consistent with clean fuel blending; namely JP-8 produces more particulates than the FT blend and far more than FT fueling (Fig. 21). The variation with JP-8 fueling is also illustrated as JP-8(2) on the figure. Less pronounced is the variation in the particulate peaking which is more consistent with that of Fig. 20.

The mean particle diameter at 175 psia (1.207 MPa) decreases with fueling blend from JP-8 to FT (Fig. 22). This trend is not evident in Fig. 20, adding to the complexity of predicting combustor particulate variations.

ENGINE EMISSIONS TESTING

Other emissions and peformance tests indicate small to no changes in emssions within limits as prescribed in the Jet A fueling specifications (Kinder and Rahmes, 2009).

A collaborative [NASA, AFRL, ARI, UTRC, and P&W] small and large on-wing engine emissions and performance test program provides several needed insights into aviations emissions (Bulzan, 2009; and NASA et al., 2008).

Small Engine Testing

Small-engine test stand observations on a test-stand-mounted PW 308 engine fueled by JP-8. FT, and FT-blended fuels

1. At low power,
   - NOx emissions are within instrument measurement capabilities
   - Lower CO emission with FT/blend may be due to higher H/C ratio

2. At intermediate or high power,
   Very low CO emissions make ratios irrelevant to evaluate differences between the fuels
   No significant difference in NOx emissions

These tests also revealed negligible unburned hydrocarbons (UHC) at all power conditions for both of the two FT fuels tested. The SO_2 emissions indicate the sulfur content of the blend to be around 50% of that for JP-8, whereas for 100% FT fuel a value of 0.1% indicates contamination. The ~2% fuel flow benefit with 100% synthetic fuel can be attributed to the higher heat content of synthetic fuel.

Approximately 2% fuel flow benefit with 100% synthetic fuel can be attributed to the higher heat content of synthetic fuel Rahmes et al. (2009) provides emissions results for an unspecified fuel that was tested in a Pratt & Whitney small turbine engine (inferred as PW 308 and biofueling). Emissions deviations were small except for core smoke (Fig. 23). The particulate distributions change with both fueling (F/A) and engine power settings, showing decreases in emissions with increses in %FT and increases with engine power setting (Figs. 24 and 25). Figure 26 provides a comparison of mean particulate diameters for JP-8, 50:50 blend, and FT fueling with changes in engine power for the PW 308 off-wing engine testing.

Large Engine On-Wing Test Results

A consortium of agencies are working together to provide on-wing engine emissions testing for 100% JP-8 or Jet A, a 50:50 blend with SPK, and 100% SPK engine fueling at various power settings. Here SPK represents different Fischer-Tropsch fuels depending on feedstock and refiner. Future testing will include biomass feedstock fueling (HRJ). For these tests the fuel was either coal- or gas-derived jet fuel. Particulate distributions given by Anderson (2009) at 30% and 65% engine power setting are provided on the left side of Fig. 27. The number of particulates and black carbon values are provided on the right side of Fig. 27.

The data presented herein show a strong dependence on F/A and blend with an implied less dependency on fuel composition. The small-engine test data figures are both normalized and too course to illustrate the dependencies for the data herein. As for the on-wing engine test results, the AAFEX program data are planned to be released in a January 2010 workshop.

These comparisons and test data presented herein imply—yet at this time cannot conclude—that sector test data replicate, at least qualitatively, on-wing test data, providing both detail and insights not gained from on-wing tests. Post AAFEX 2010 Workshop analysis of released data and data herein is warranted.

CONCLUSIONS: PART B

Alternate fueling testing is being carried out to determine preliminary performance, emissions, and particulates combustor sector data relative to JP-8+100 as baseline fueling, for SPK-type (e.g., Fischer-Tropsch, FT) fuels blends and projections for testing of biofuel fuel blends leading to preliminary development of smart fueling (fuel flexible) and combustor systems for the next generation aeronautic and aeronautic-derivative gas turbine engines. Herein alternate fueling test results for a well characterized but proprietary combustor are provided for JP-8+100, a FT-derived fuel, and a blend of 50% each by volume.

The test data presented are part of a more extensive data set where combustion parameters were varied over a range of values. The data herein are for the case of nominal inlet conditions at 75 psia (0.517 MPa) to 225 psia (1.551 MPa) and 800 °F (700 K), and JP-8+100 is taken as the baseline.

1. The 50:50 blend test performance and emission results generally are between JP and FT and somewhat closer to FT
2. Emissions: CO is lower with FT; CO_2 is about the same; NO is lower with FT; NO_2 is higher with FT fueling F/A; NOx is lower to higher with FT with F/A; O_2 decreases with F/A (consistent with temperature increase), is lower with FT with increased spread from JP-8 with F/A, again consistent with rake temperature; HC generally decreases with F/A, yet FT humps at 0.015. No explanation is provided.
3. Basic emissions show more change with F/A than with JP-8 or FT; the latter being the more significant. These results appear to agree qualitatively to on-wing engine testing. Quantitative agreement requires resolution pending data release. The other aspect is to look at how emissions change with pressure and EXTRAPOLATE those results to core pressure on the ground, that is, at much higher pressures.
4. Comparisons of engine on-wing and combustor-sector test data imply (but not conclude at this time) replication. Post AAFEX 2010 Workshop data analysis is warranted.

REFERENCES

Anderson, B., 2009, "Langley Aircraft Emission Research: Highlights and Overview of the Alternative Aviation Fuel Experiment," AMRD/AAFEX program presentation, NASA Langley Research Center, Hampton, VA.

Bulzan, D., 2009, "Alternative Aviation Fuel Experiment (AAFEX): Overview," NASA Glenn Research Center, Cleveland, OH.

Hendricks, R. C., Shouse, D. T., Roquemore, W. M., Burns, D. L., Duncan, B. S., Ryder, R. C., Brankovic, A., Liu, N.-S, Gallagher, J. R., and Hendricks, J. A., 2004, "Experimental and Computational Study of Trapped Vortex Combustor Sector Rig With Tri-Pass Diffuser," NASA/TM—2004-212507, NASA Glenn Research Center, Cleveland, OH.

Kinder, J. D., and Rahmes, T., 2009, "Evaluation of Bio-Derived Synthetic Paraffinic Kerosenes (Bio-SPK)," Sustainable Biofuels Research & Technology Program document, The Boeing Company, Seattle, WA.
http://www.boeing.com/aboutus/govt_ops/reports_white_papers/pas_biofuel_exec_summary.pdf

NASA, AFRL, ARI, UTRC, and P&W, 2008, "Alternative Fuel Test on PW308 Engine," collaborative presentation.

Rahmes, T. F., Kinder, J. D., Henry, T. M., Crenfeldt, G., LeDuc, G. F., Zombanakis, G. P., Abe, Y., Lambert, D. M., Lewis, C., Juneger. J. A., Andac, M. G., Reilly, K. R., Holmgren, J. R., McCall, M. J., and Bozzano, A. G., 2009, "Sustainable Bio-Derived Synthetic Paraffinic Kerosene (Bio-SPK) Jet Fuel Flights and Engine Tests Program Results," AIAA 2009–7002, *9th AIAA Aviation Technology, Integration, and Operation Conference (ATIO)*, AIAA, Reston, VA.

Shouse, D. T., Stutrud, J. S., and Frayne, C. W., 2001, "High Pressure Combustion Research at the Air Force Research Laboratory," ISOABE–2001–1119, Fifteenth International Symposium on Air Breathing Engines, Bangalore, India.

Table. 1 Variations in combustor efficiencies with F/A and fueling composition for nominal inlet conditions at 225 psia (1.551 MPa) and 800 °F (700 K) with JP-8 +100 as baseline.[a] Combustor pressure drop ~3%

F/A	JP-8 +100	JP-8:FT 50:50 blend	FT
	F	H	G
0.010	99.89	99.9	99.91
	O	K	M
0.015	99.93	99.94	99.91
	Q	U	T
0.020	99.94	99.94	99.95
0.025			

[a]Letters refer to proprietary data reduction parameters

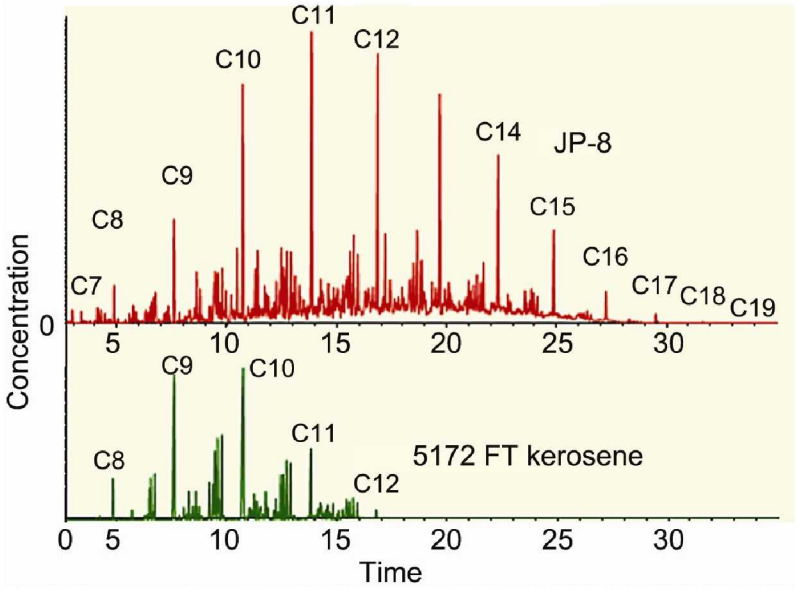

Fig. 1a Representative carbon distributions for JP-8 and AFRL No. 5172 FT (SPK) from Shell gas-to-liquid (GTL) with 0% aromatics and 0% sulfur. The JP-8 cited is 19% aromatics and 1200 ppm sulfur

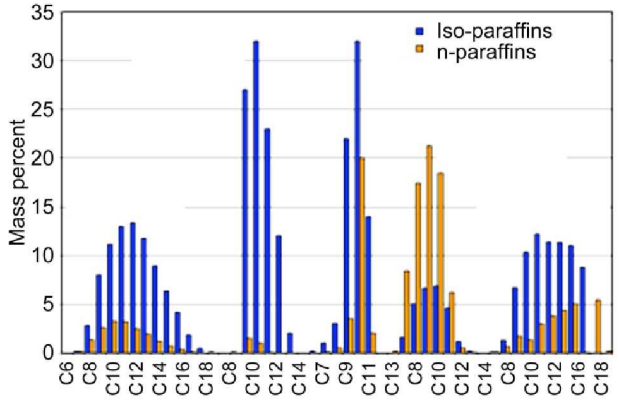

Fig. 1b Variations in representative carbon distributions for proposed alternate fuels with high and low n-paraffinic to isomer ratios

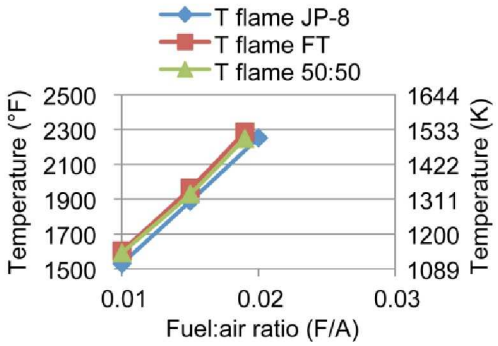

Fig. 2 Calculated flame temperature variation (°F) with F/A and fuel composition

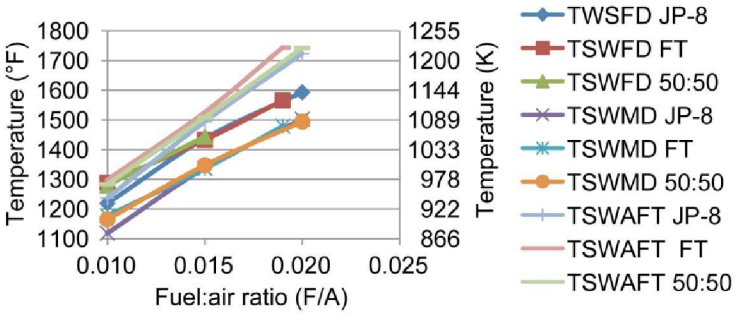

Fig. 3 Sidewall temperature variation (°F) with F/A and fuel composition

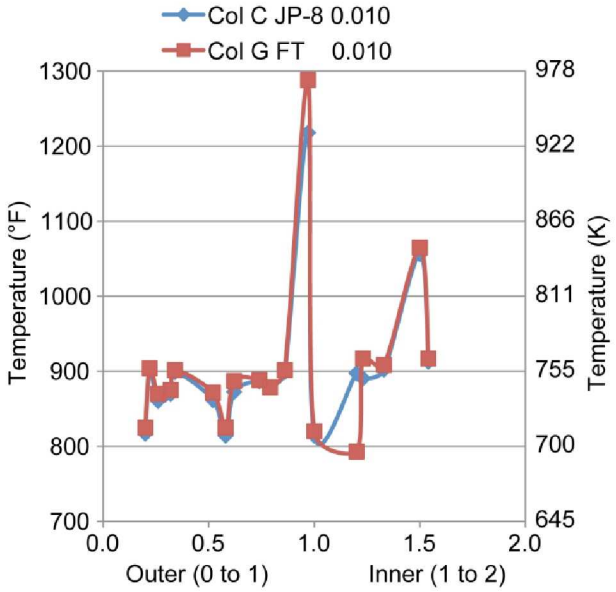

Fig. 4a Unwrapped liner temperatures (°F) for F/A = 0.010 and fueling compositions JP-8 and FT. Normalized combustor liner thermocouple locations: 0 to 1 outer and 1 to 2 inner

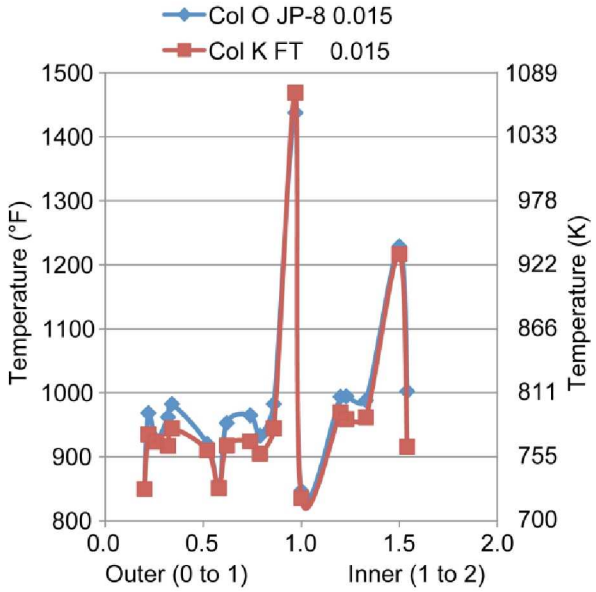

Fig. 4b Unwrapped liner temperatures (°F) for F/A = 0.015 and fueling compositions JP-8 and FT. Normalized combustor liner thermocouple locations: 0 to 1 outer and 1 to 2 inner

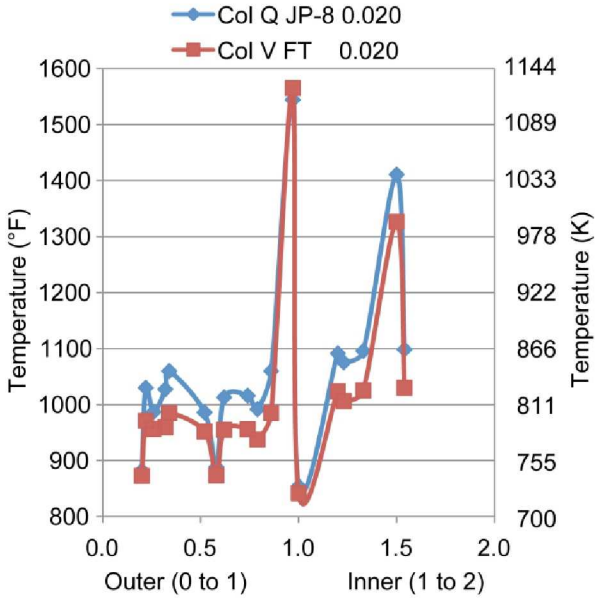

Fig. 4c Unwrapped liner temperatures (°F) for F/A ~ 0.020 and fueling compositions JP-8 and FT. Normalized combustor liner thermocouple locations: 0 to 1 outer and 1 to 2 inner

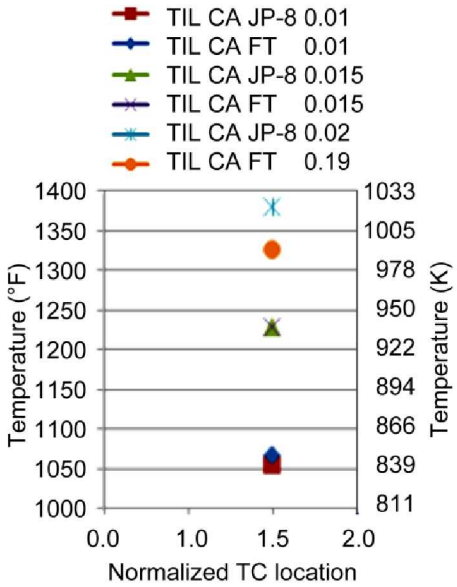

Fig. 5 Peak inner liner temperatures (TIL) (°F) at normalized location 1.5

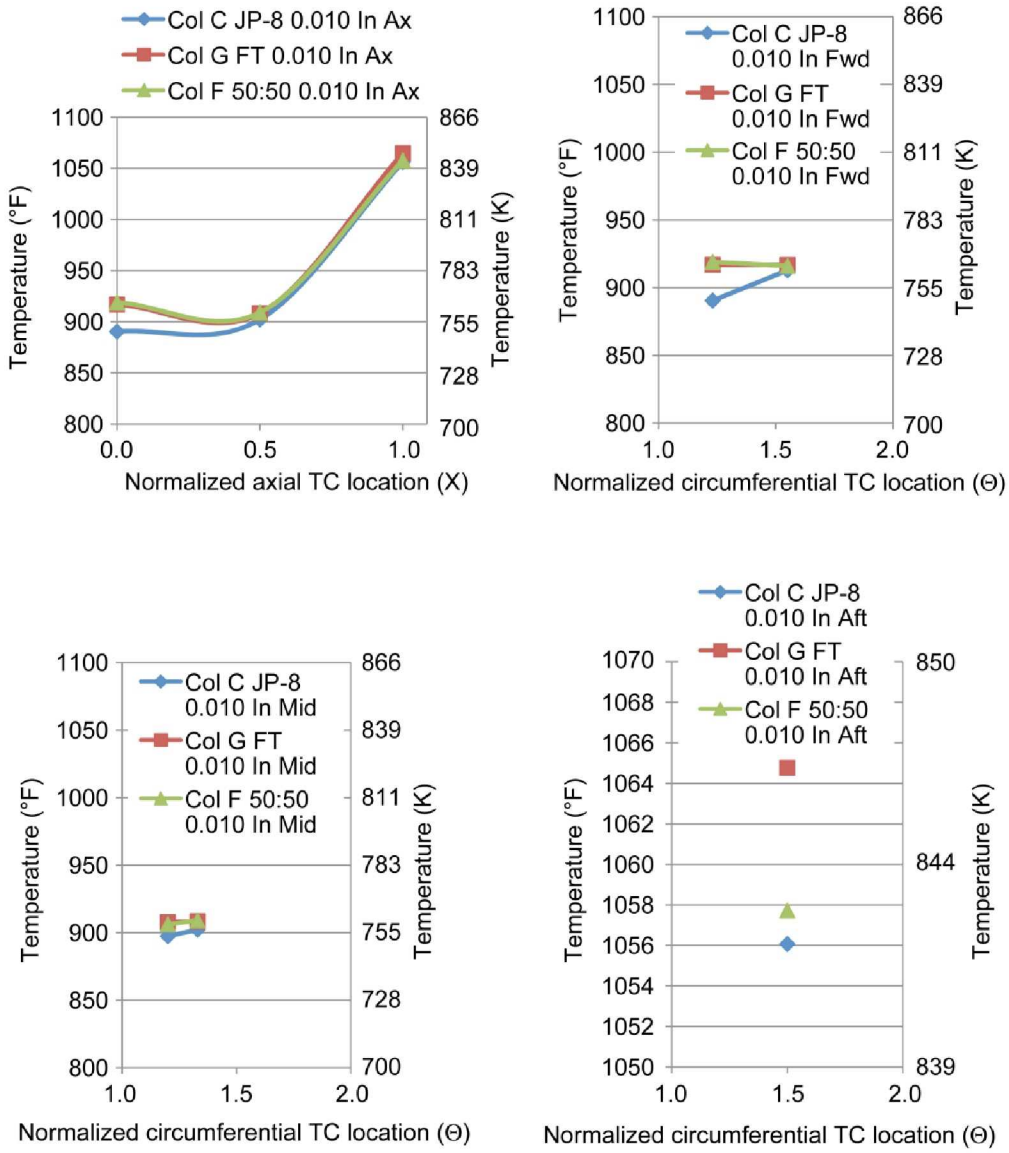

Fig. 6a Combustor liner inner surface temperature variations (°F) with fueling composition at F/A = 0.010

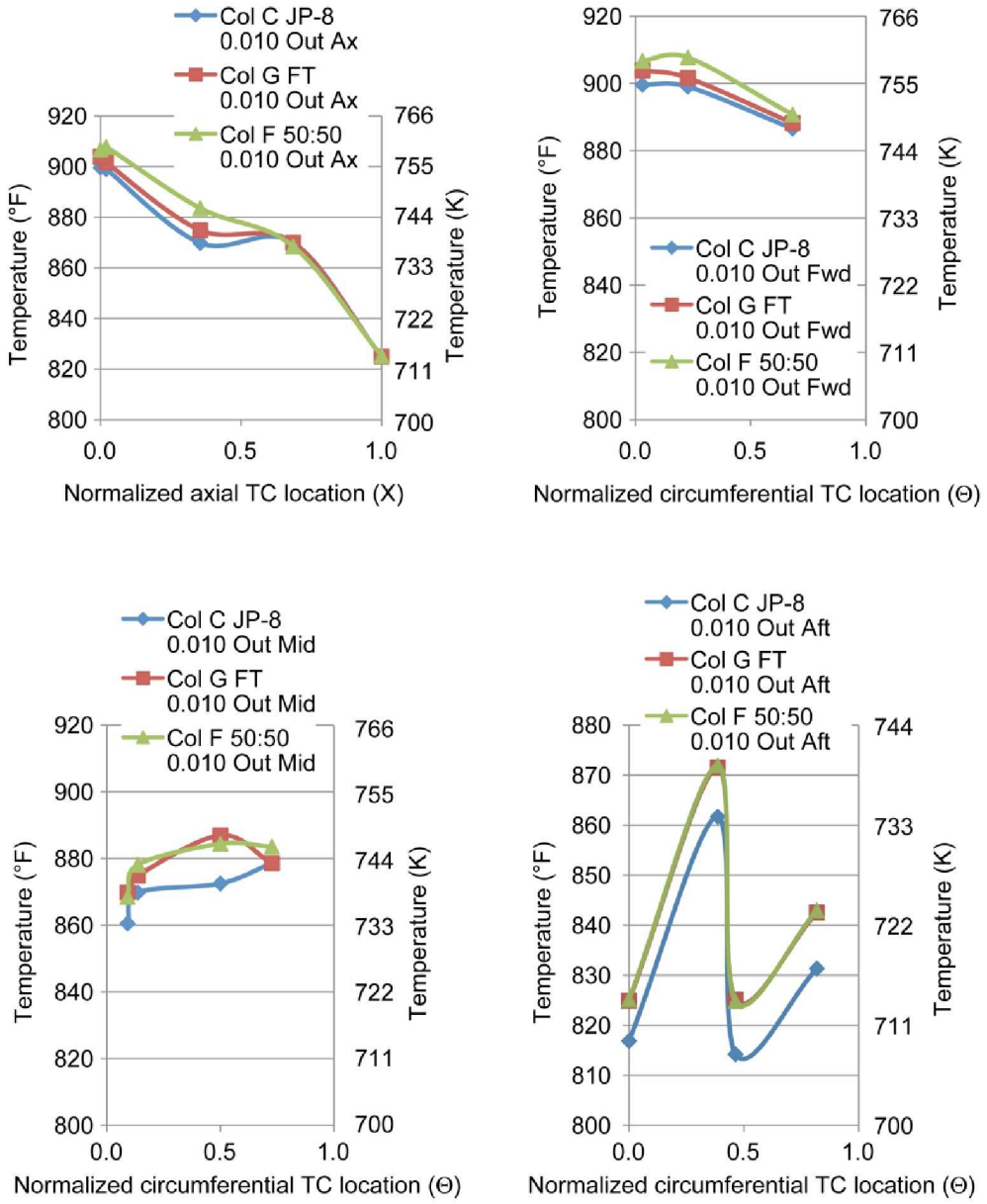

Fig. 6b Combustor liner outer surface temperature variations (°F) with fueling composition at F/A = 0.010

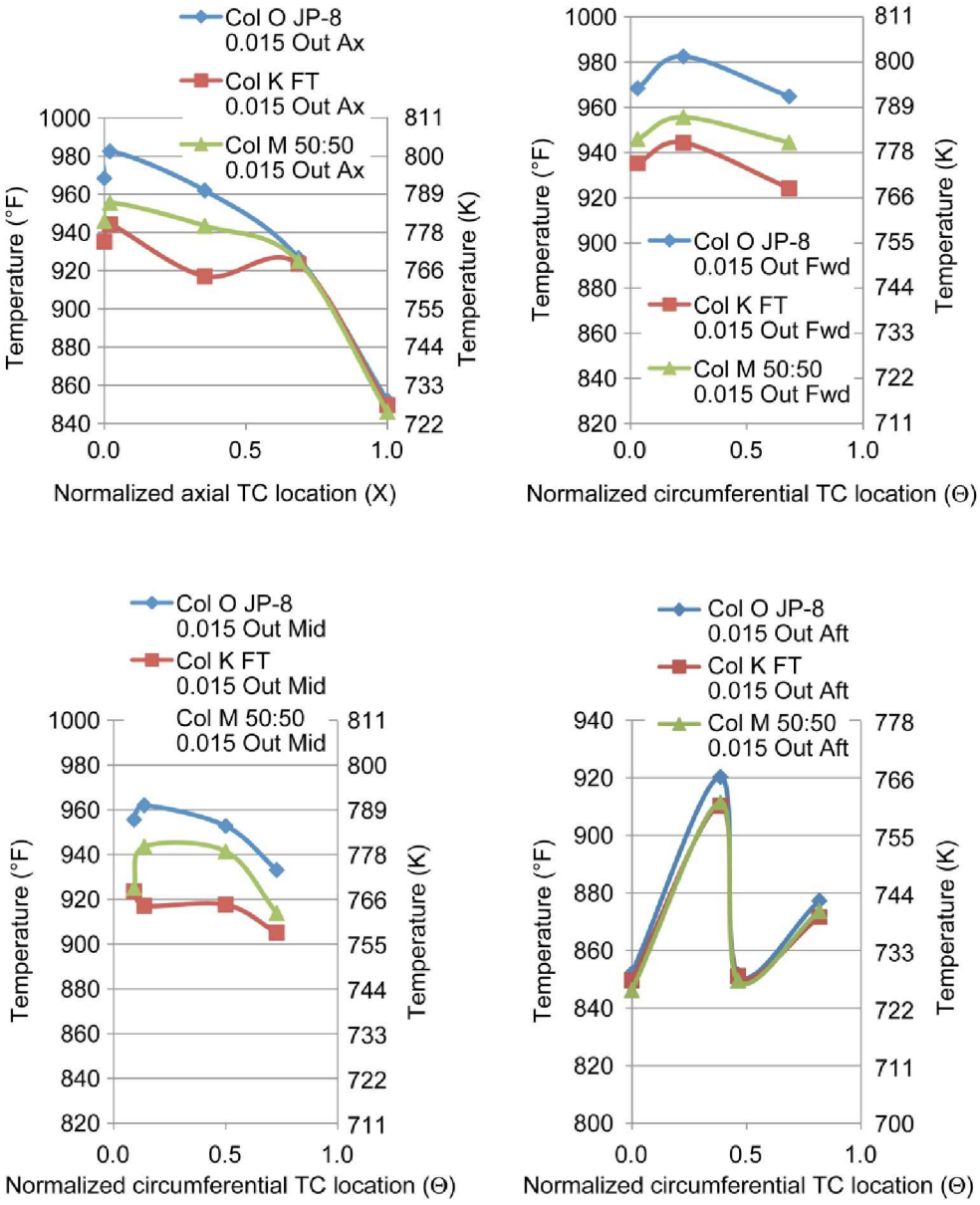

Fig. 6c Combustor outer liner temperature variations (°F) with fueling composition at F/A = 0.015

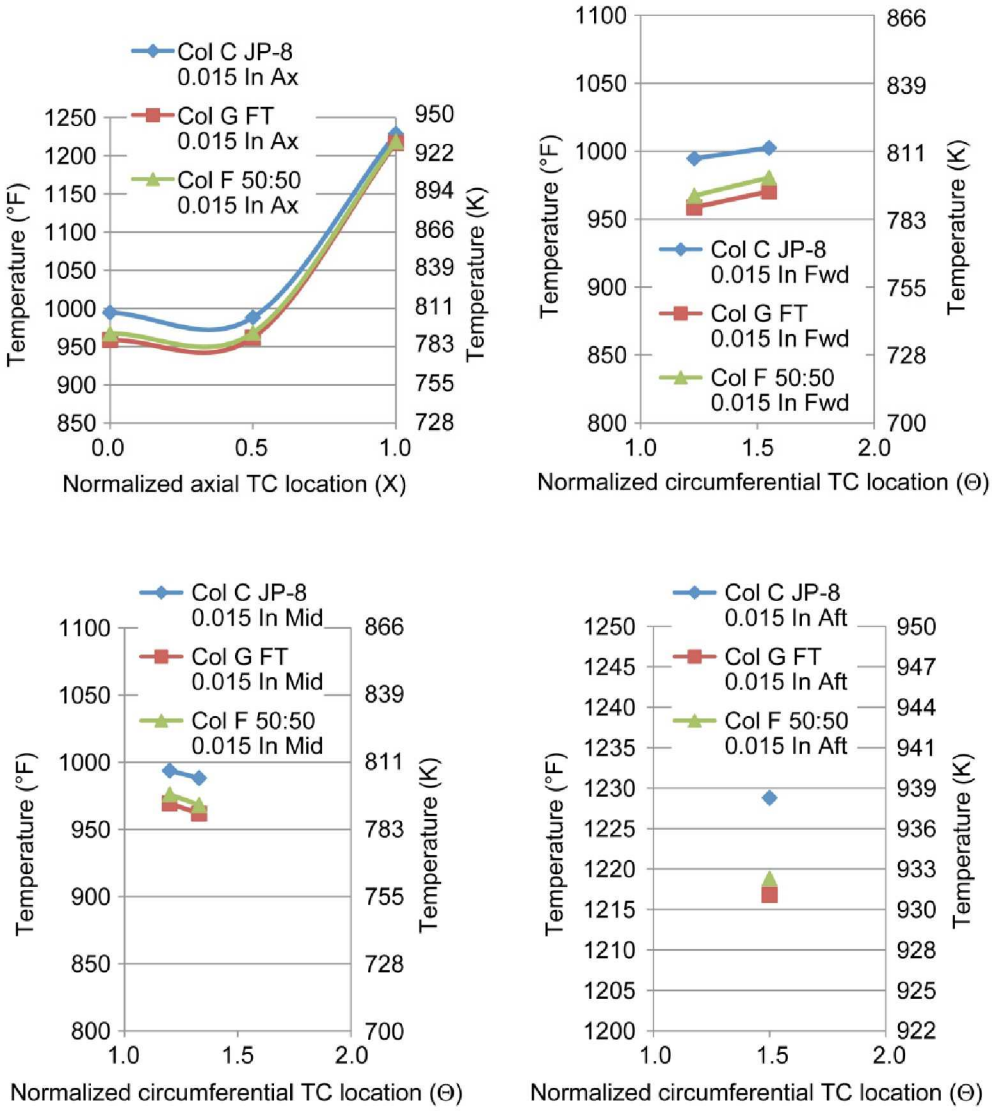

Fig. 6d Combustor inner liner temperature variations (°F) with fueling composition at F/A = 0.015

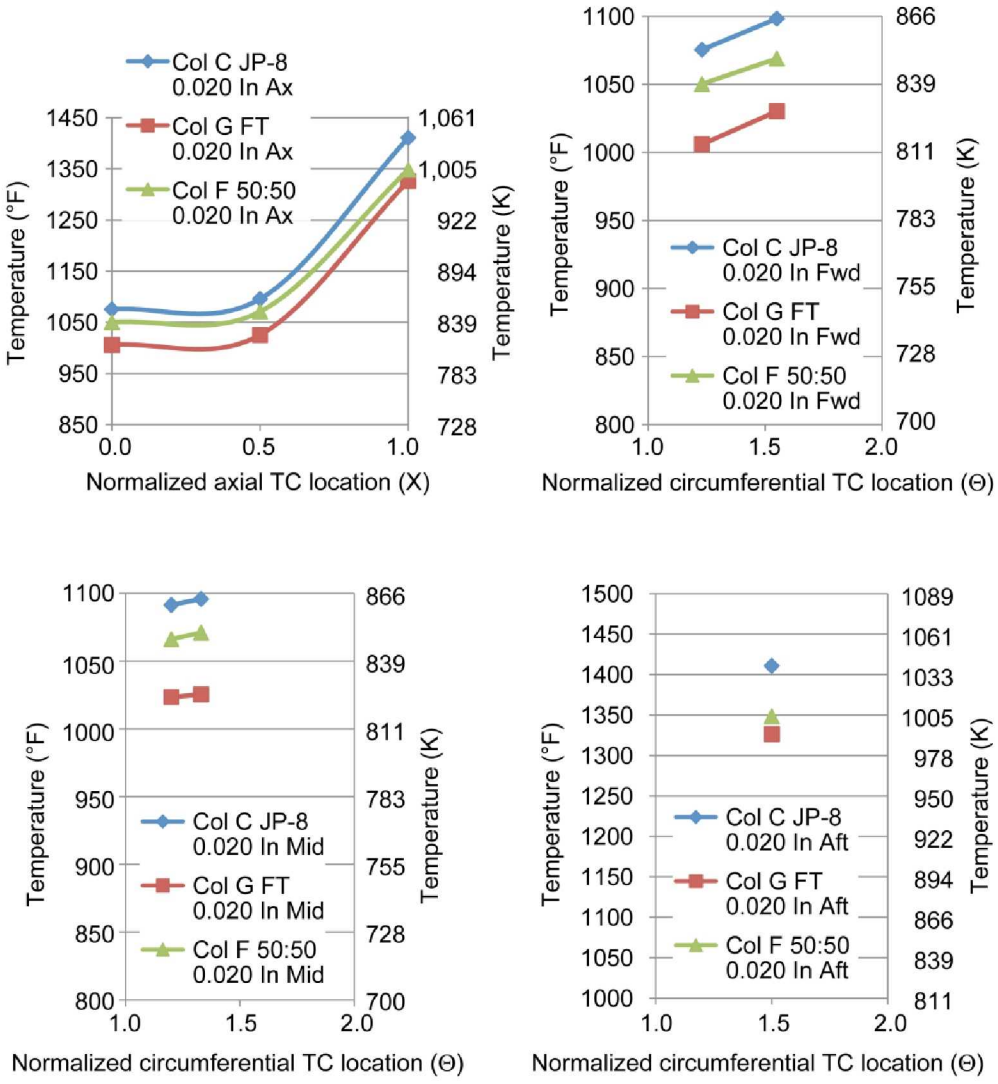

Fig. 6e Combustor inner liner temperature variations (°F) with fueling composition at F/A ~0.020

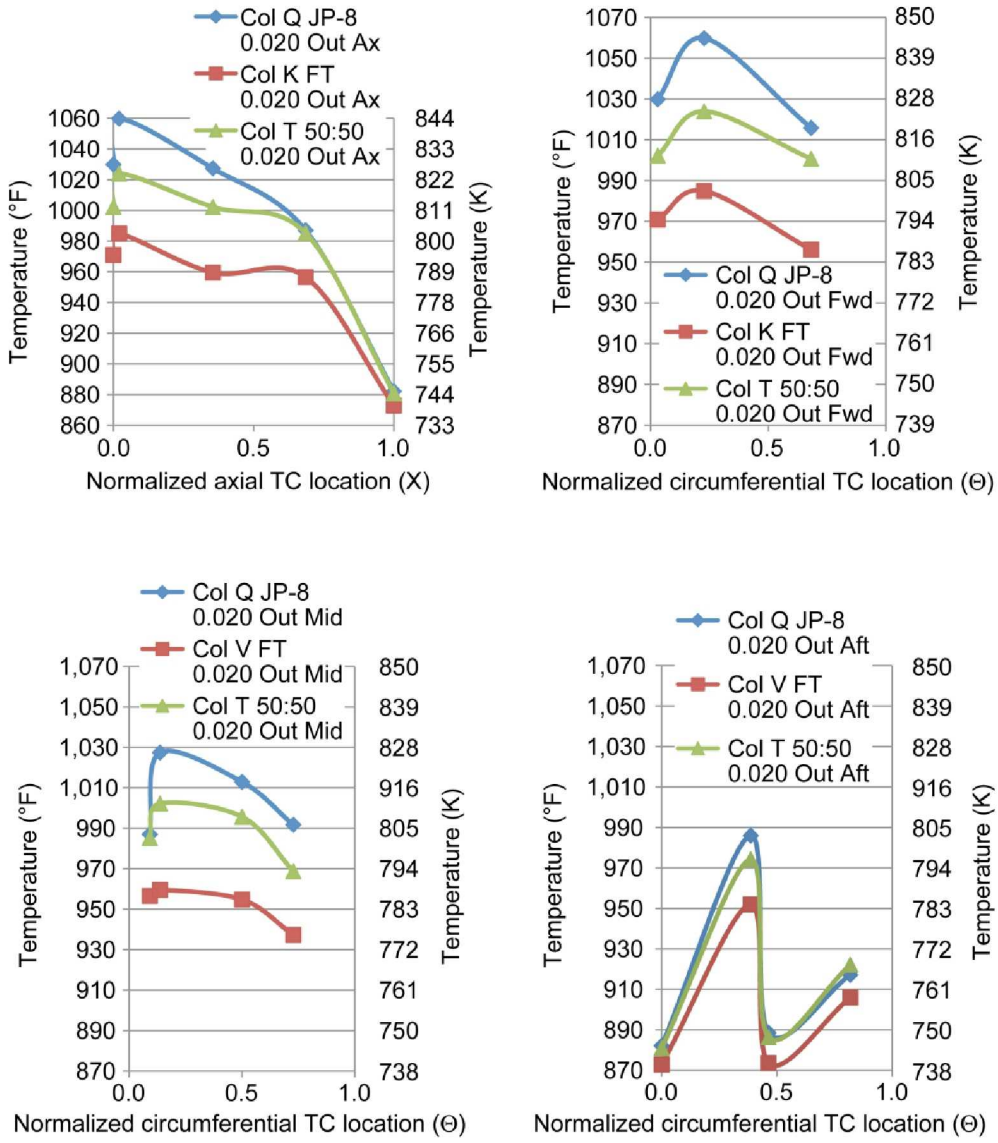

Fig. 6f Combustor outer liner temperature variations (°F) with fueling composition at F/A ~0.020

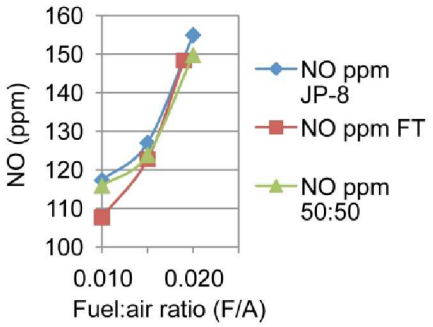

Fig. 7a Nitric oxide emission (ppm) variations with F/A and fueling composition

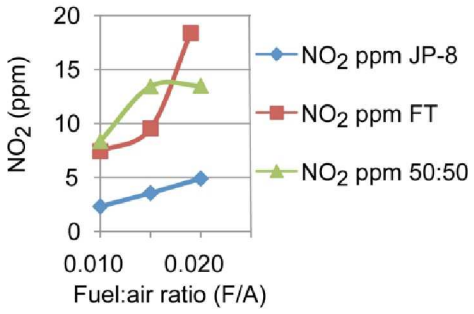

Fig. 7b Nitrogen dioxide emission (ppm) variations with F/A and fueling composition

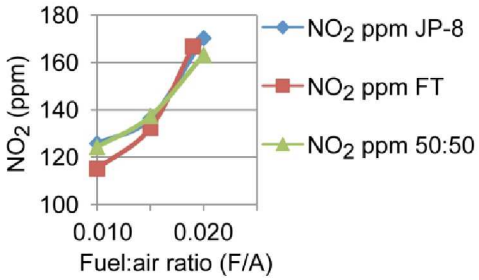

Fig. 7c NOx emission variations (ppm) with F/A and fueling composition

[(g/kg) [EINOx or KHNOx] ≈ (ppm NOx) (1 + FAR)/(630 FAR)]. FAR = fuel:air ratio F/A (Hendricks et al., 2004)
[(g/kg) [EINOx or KHNOx] ≈ (ppm NOx) (1 + FAR)/(715 FAR)]. FAR = fuel:air ratio F/A (herein, arp)
[(g/kg) [EINOx or KHNOx] ≈ (ppm NOx) (1 + FAR)/(655 FAR)]. FAR = fuel:air ratio F/A (herein, arpc)
Aerospace recommended practice (arp) and (arpc) corrected arp
$EI_Z \approx [10^3 m_Z/m_f] \times [m_f (1+FAR^{-1})/m_{\text{gas products}}] \times [mol_Z M_Z/m_Z] \times [m_{\text{gas products}}/(\sum mol_j M_j)_{\text{gas products}}] \times 10^3/10^3 \times 10^{-6}$ ppm
m_X = mass flow rate $_X$ (g/s), m_f = mass flow rate of fuel (kg/s), M_X = mol mass$_X$, mol$_X$ = moles $_X$, FAR = fuel:air ratio F/A
[(g/kg) [EINOx] SAE ARP 1533 ~ $(\{[NOx]/([CO]+[CO_2] + [C_xH_y]\} \times 10^3 M_{NOx}/(M_C + \alpha M_H)$
[NOx] [CO] [CO_2] [C_xH_y] = mass fractions of NOx, CO, CO_2, and total hydrocarbon THC, M = molar mass, α = ratio of H/C = n/m in fuel C_mH_n where NOx mol mass is assumed to be 46; contrast to Figs. 7a and 7b

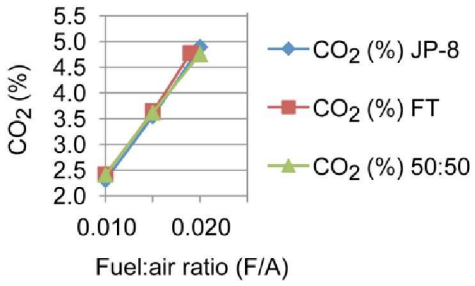

Fig. 8 Variation of %CO2 with F/A and fuel composition

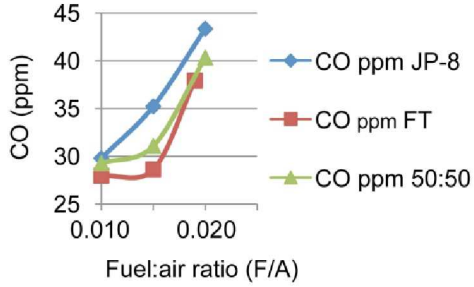

Fig. 9 Variation of CO (ppm) with F/A and fuel composition. [(g/kg) EICO ≈ (ppm CO) (1+ FAR)/(1220 FAR)]. FAR = fuel:air ratio F/A

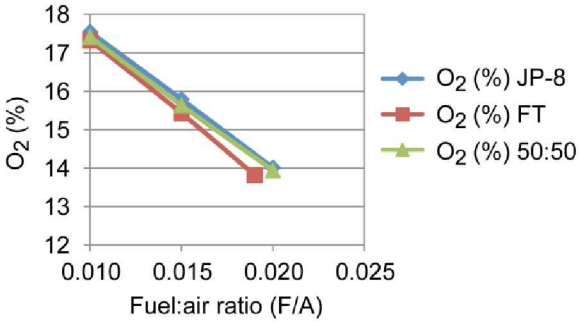

Fig. 10 Variation of $\%O_2$ with F/A and fuel composition

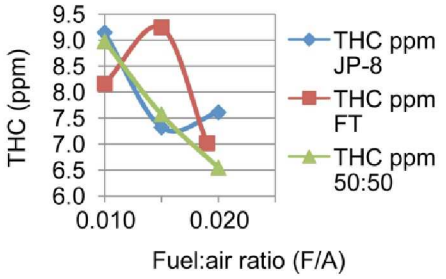

Fig. 11 Total hydrocarbon variations, THC (ppm) with F/A and fuel composition. [(g/kg) THC ≈ (ppm THC) (1+ FAR)/(2070 FAR)]. FAR = fuel:air ratio F/A

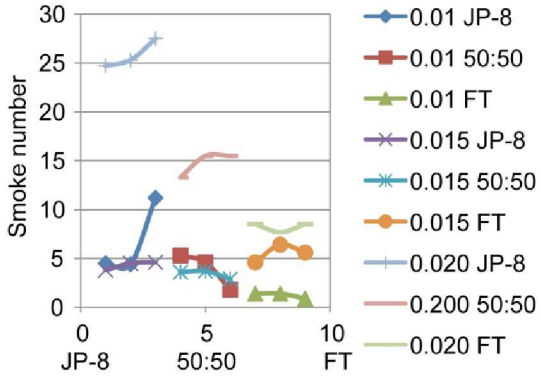

Fig. 12 Smoke number variations with F/A and fueling composition

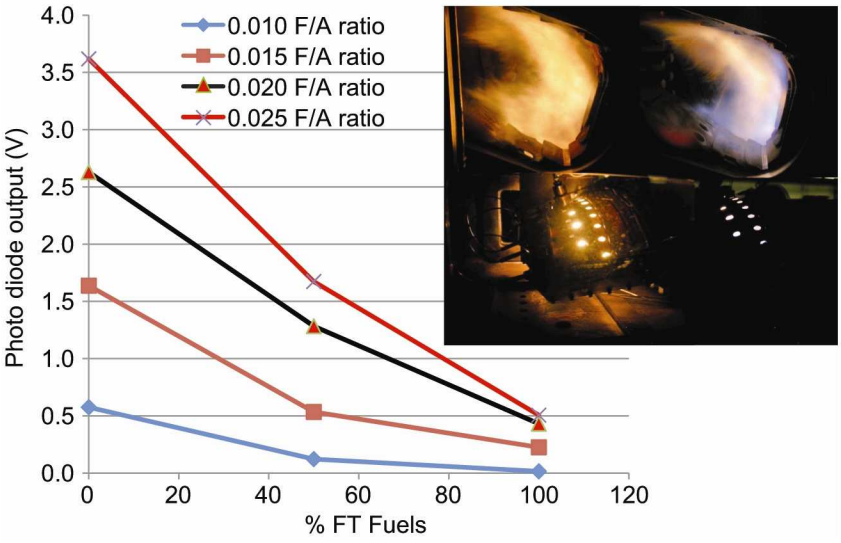

Fig. 13 Variation in photo diode voltage output with fuel blending at various F/A ratios for 100% JP-8 and 100% FT fueling as well as 50% blend of JP-8 and FT fuel; $(P,T)_{inlet}$ is [75 psia (0.517 MPa), 500 °F (533 K)] at 3% combustor pressure drop. Photo on left is 100% JP-8 and on the right 100% FT at F/A =0.010

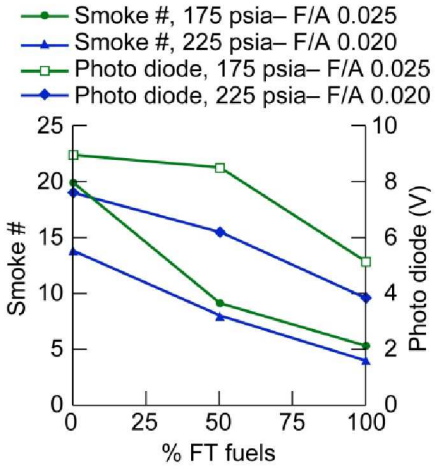

Fig. 14 Smoke number variations with %FT fueling for combustor inlet pressures of 175 and 225 psia (1.207 and 1.551 MPa) at F/A = 0.020 and 0.025. Results imply reductions in polycyclic aromatic hydrocarbons (PAH) (soot) and polycyclic aromatic compounds (PAC).

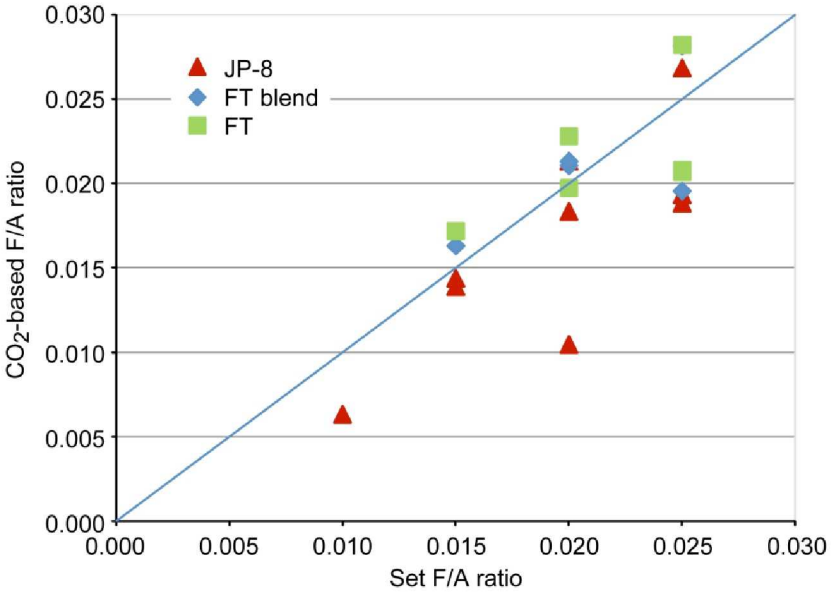

Fig. 15 Alternate fuel experimentally set F/A versus CO_2-based calculated F/A

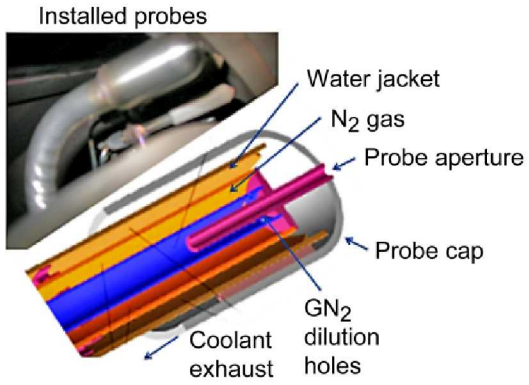

Fig. 16. Emissions probes installed at combustor exhaust exit plane. Particulate probe is in photo foreground with gas emissions/TC rake probes in background. Details of the water cooled, nitrogen gas dilution particulate probe shown in inset. Probe cap outer diameter = 0.075 in. (19 mm) with aperture diameter 0.044 in. (1.12 mm). Both diluted and undiluted probes were installed. Photo of installed probes shown rotated out of true combustor exhaust plane position.

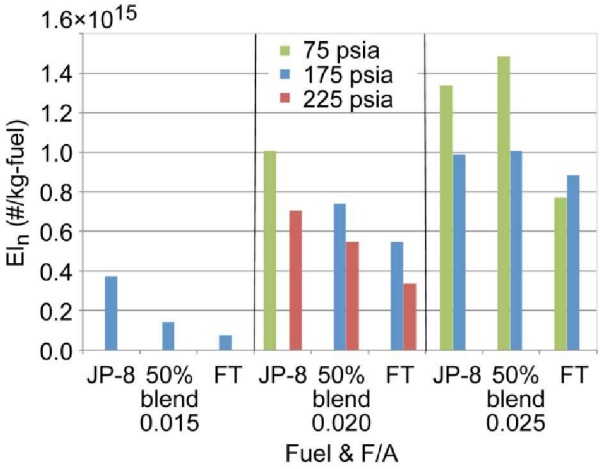

Fig. 17 Particulate emissions number indices variations with test pressure and F/A for JP-8, FT blend, and FT fueling.

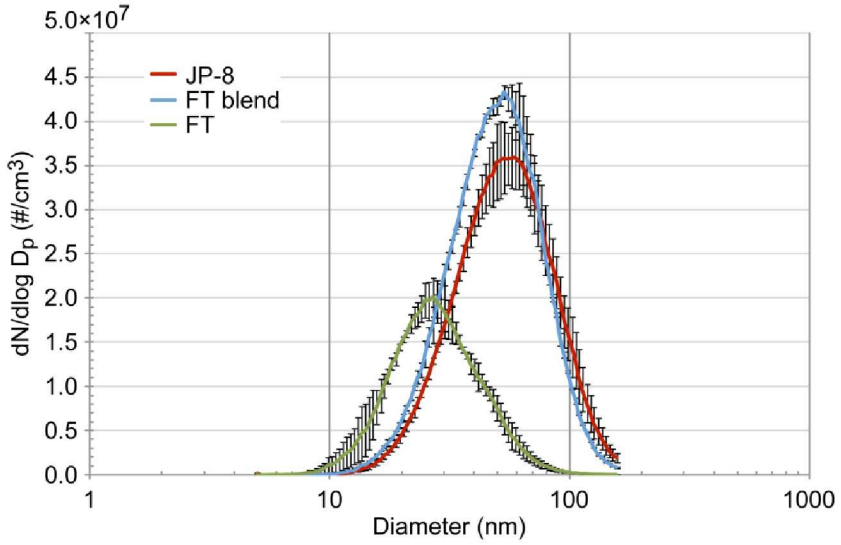

Fig. 18 Alternate fueling particle size distribution with JP-8, FT blend, and FT for combustor pressure at 75 psia (0.517 MPa) and F/A = 0.025. $dEI/d(\log Dp) = 2.833\times10^3$ [dN/d(log Dp)][(1+ FAR)/FAR](T/P) where N = number/cm^3, EI = number/kg, and FAR = fuel:air ratio F/A; P is instrument pressure in atmospheres and T is temperature in K (herein 1 atm and ~293 K)

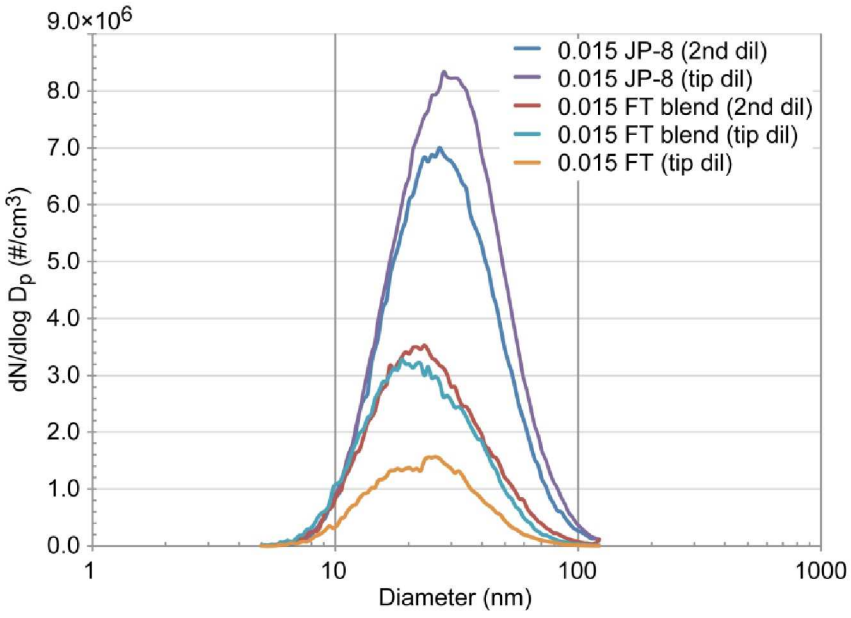

Fig. 19 Particulate size distribution changes with probe dilution with JP-8, FT blend, and FT fuels for combustor pressure 125 psia (0.862 MPa) and F/A = 0.015. $dEI/d(\log Dp) = 2.833\times10^3$ [dN/d(log Dp)][(1+ FAR)/FAR](T/P) where N = number/cm^3, EI = number/kg, and FAR = fuel:air ratio F/A; P is instrument pressure in atmospheres and T is temperature in K (herein 1 atm and ~293 K)

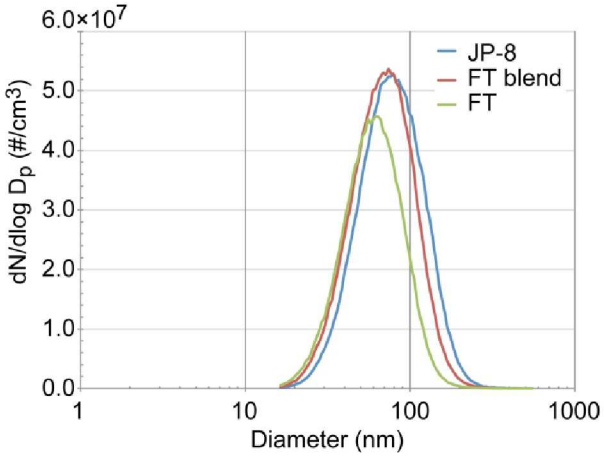

Fig. 20 Particle size distribution with JP-8, FT blend, and FT for combustor pressure 175 psia (1.207 MPa) and F/A = 0.025. dEI/d(log Dp) = 2.833×10^3 [dN/d(log Dp)][(1 + FAR)/FAR](T/P) where N = number/cm^3, EI = number/kg, and FAR = fuel:air ratio F/A; P is instrument pressure in atmospheres and T is temperature in K (herein 1 atm and ~293 K)

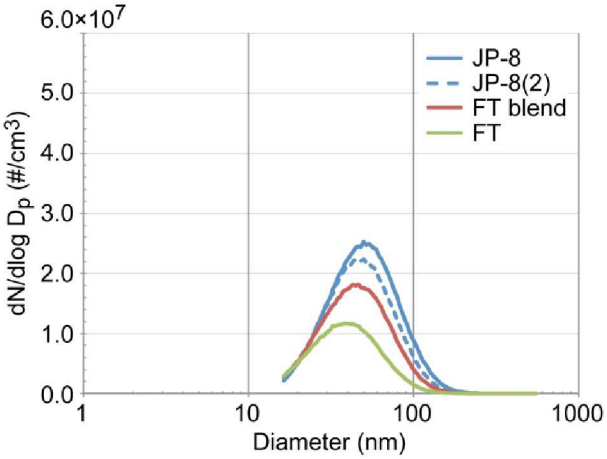

Fig. 21 Particulate size distribution for JP-8, FT blend, and FT fueling at combustor pressure 225 psia (1.551 MPa) and F/A = 0.020. dEI/d(log Dp) = 2.833×10^3 [dN/d(log Dp)][(1 + FAR)/FAR](T/P) where N = number/cm^3, EI = number/kg, and FAR = fuel:air ratio F/A; P is instrument pressure in atmospheres and T is temperature in K (herein 1 atm and ~293 K)

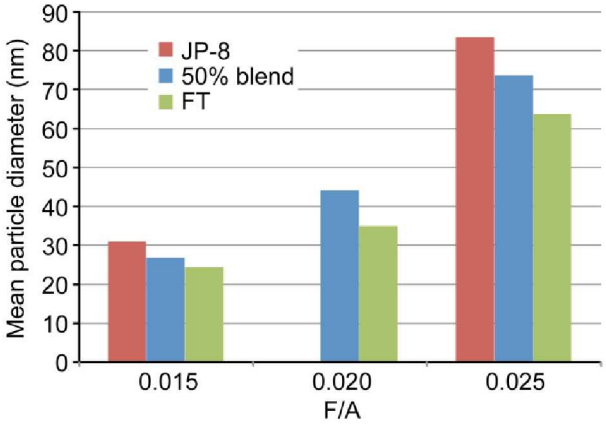

Fig. 22 Mean particle diameter with JP-8, FT blend, and FT fueling for combustor pressure 175 psia (1.207 MPa) and F/A ratios of 0.015, 0.020, and 0.025

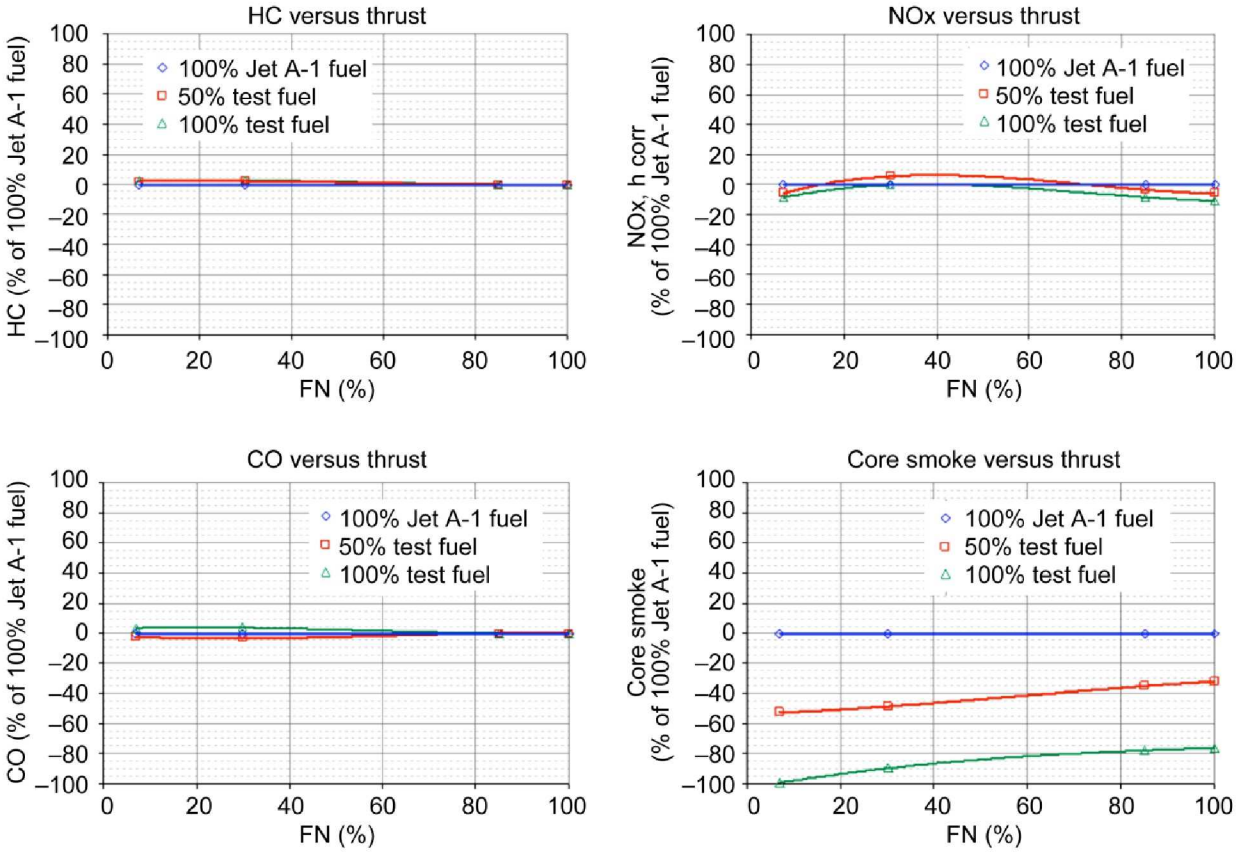

Fig. 23 Small turbine engine emissions test results (Rahmes et al., 2009)

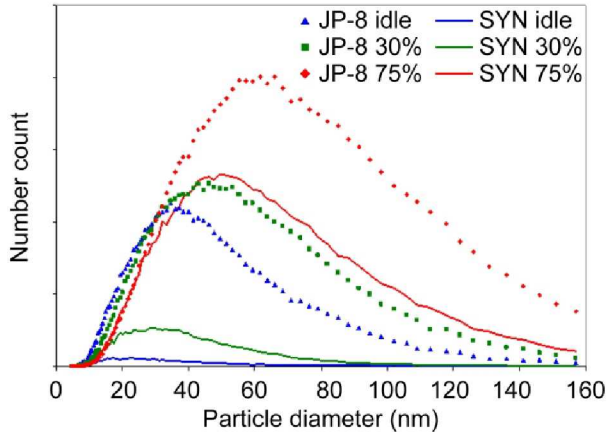

Fig. 24 Variation of particulate distribution with fueling changes (alternative fuels PW 308 engine testing)

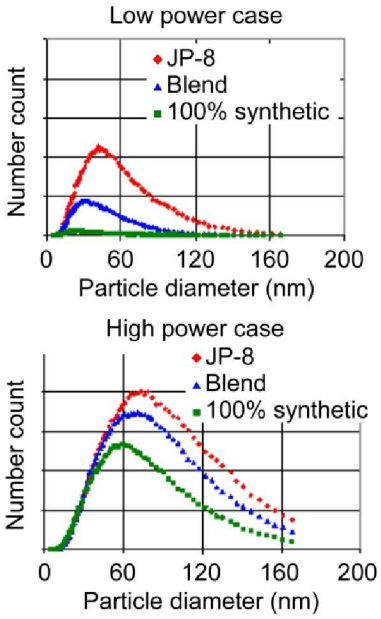

Fig. 25 Changes in particulate distribution with power and fueling (alternative fuels PW 308 engine testing)

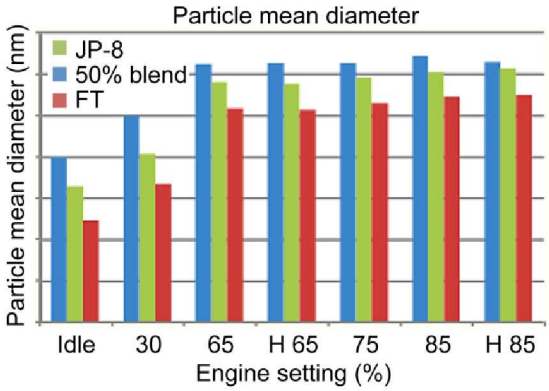

Fig. 26 Variations of mean particulate diameter with fueling and power level (alternative fuels PW 308 engine testing)

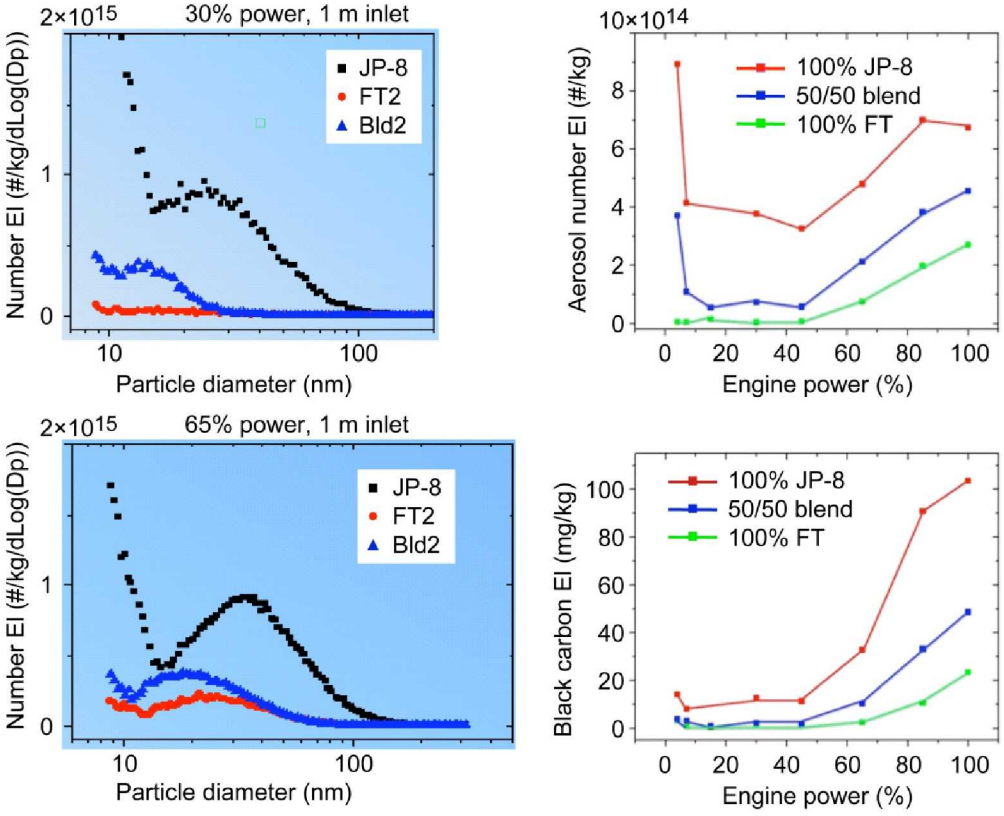

Fig. 27 On-wing engine emissions testing measurements for particulates with JP-8, 50:50 JP-8 and S8 blend, and 100% S8, where S8 represents an FT fueling with either coal- or gas-derived jet fuel (Anderson, 2009)

APPENDIX A: Table of fuel specifications (AFRL No. 5172)

Fuel specifications

Method	Test	Result
ASTM D 3242–05	Total acid number (mg KOH/g)	0.002
ASTM D 1319–05	Aromatics (% vol)	0.0
ASTM D 3227–04a	Mercaptan sulfur (% mass)	0.000
ASTM D 4294–03	Total sulfur (% mass)	0.00
ASTM D 86–07a	Distillation	
	Initial boiling point (°C)	148
	10% recovered (°C)	162
	20% recovered (°C)	163
	50% recovered (°C)	169
	90% recovered (°C)	185
	End point (°C)	198
	Residue (% vol)	0.9
	Loss (% vol)	1.1
ASTM D 93–07	Flash point (°C)	44
ASTM D 4052–96	API gravity @ 60 °F	60.5
ASTM D 5972–05	Freezing point (°C)	–54
ASTM D 445–06	Viscosity @ –20 °C (mm^2/s)	2.6
ASTM D 3338–05	Net heat of combustion (MJ/kg)	44.2
ASTM D 3343–05	Hydrogen content (% mass)	15.6
ASTM D 1322–97	Smoke point (mm)	40.0
ASTM D 130–04	Copper strip corrosion (2h @ 100 °C)	1a
ASTM D 3241–06	Thermal stability @ 260 °C	
	Change in pressure (mmHg)	0
	Tube deposit rating, visual	1
ASTM D 381–04	Existent gum (mg/100 mL)	<1
ASTM D 5452–06	Particulate matter (mg/L)	0.5
MIL–DTL–83133E	Filtration time (min)	3
ASTM D 1094–00	Water reaction interface rating	1
ASTM D 5006–03	FSII (% vol)	0.00
ASTM D 2624–07	Conductivity (pS/m)	233
ASTM D 5001–06	Lubricity test (BOCLE) wear scar (mm)	0.77
ASTM D 4809–06	Net heat of combustion (MJ/kg)	44.2
MIL–DTL–83133E	Workmanship	Pass

APPENDIX B: Table of combustor outer and inner liner temperature data

Combustor outer and inner liner temperature (°F) data for F/A = 0.010, 0.015, 0.020, and nominal inlet pressure 225 psia (1.55 MPa), 800 °F (700 K) at 3% combustor pressure drop

				F/A = 0.010			F/A = 0.015			F/A = 0.020		
	Unwrap			JP-8	FT	50:50	JP-8	FT	50:50	JP-8	FT	50:50
TC	TC No.	X	Θ	Col C	Col G	Col F	Col O	Col K	Col M	Col Q	Col V	Col T
Outer liner												
			0.00									
TOLAL	22	0.94	0.20	817	825	825	852	850	846	882	873	881
TOLFL	20	0.00	0.22	900	904	907	968	935	946	1030	971	1002
TOLML	21	0.67	0.26	861	870	869	927	924	925	987	957	985
TOLMWA	24	0.19	0.32	870	875	878	962	917	944	1027	960	1002
TOLFM	27	0.00	0.34	899	902	908	983	944	956	1060	985	1024
TOLCA	25	1.00	0.52	862	872	872	920	910	912	986	952	974
TOLAM	28	0.94	0.58	814	825	825	852	851	850	888	874	886
TOLMR	36	0.67	0.62	873	887	884	953	918	941	1013	955	996
TOLFR	34	0.00	0.74	887	888	891	965	924	944	1016	956	1001
TOLMWI	23	0.33	0.79	879	879	884	933	905	914	992	937	969
TOLAR	37	0.84	0.86	831	843	843	877	872	874	917	906	922
TSWFD	41	0.22	0.97	1218	1288	1280	1438	1469	1444	1544	1565	1581
TSWFT	30	0.78	1.00	814	820	820	847	836	841	854	842	850
Inner liner												
TILMWI	38	0.50	1.20	897	793	906	994	969	976	1091	1023	1066
TILFR	35	0.00	1.23	890	917	919	995	959	967	1075	1006	1050
TILMWO	26	0.50	1.33	902	908	909	988	962	968	1096	1025	1071
TILCA	29	1.00	1.50	1056	1065	1058	1229	1217	1219	1411	1326	1348
TILFL	39	0.00	1.54	913	917	916	1002	916	981	1098	1030	1069
			2.00									